Improving flame retardancy of in-situ silica-epoxy nanocomposites cured with aliphatic hardener: Combined effect of DOPO-based flame-retardant and melamine

(Article begins on next page)

16 July 2022

Improving flame retardancy of in-situ silica-epoxy nanocomposites cured with aliphatic hardener: Combined effect of DOPO-based flame-retardant and melamine

Aurelio Bifulco [a,b], Dambarudhar Parida [b], Khalifah A. Salmeia [b,c], Sandro Lehner [b], Rolf Stämpfli [d], Hilber Markus [b], Giulio Malucelli [e,*], Francesco Branda [a,*], Sabyasachi Gaan [b,*]

[a] Department of Chemical Materials and Industrial Production Engineering (DICMaPI) University of Naples Federico II, Naples, Italy

[b] Laboratory for Advanced Fibers, Empa Swiss Federal Laboratories for Materials Science and Technology, Lerchenfeldstrasse 5, 9014 St., Gallen, Switzerland

[c] Department of Chemistry, Faculty of Science, Al-Balqa Applied University, 19117 Al-Salt, Jordan

[d] Laboratory for Biomimetic Membranes and Textiles, Empa Swiss Federal Laboratories for Materials Science and Technology, Lerchenfeldstrasse 5, 9014 St., Gallen, Switzerland

[e] Department of Applied Science and Technology, Politecnico di Torino, Viale Teresa Michel 5, Alessandria 15121, Turin, Italy

ARTICLE INFO

ABSTRACT

Silica-epoxy nanocomposites were prepared via an "in-situ" sol-gel synthesis process and a phosphorus (P) flame-retardant i.e. 6H-dibenz[c,e][1,2]oxaphosphorin,6-[(1-oxido-2,6,7-trioxa-1-phosphabicyclo[2.2.2]oct-4-yl)methoxy]-, 6-oxide (DP) and melamine (Mel) were further added to the matrix to improve its fire performance. The main components of epoxy resin were bisphenol A diglycidyl ether (DGEBA) and isophorone diamine (IPDA) hardener. The addition of DP as well as silica alone into the epoxy system stopped the melt dripping phenomena in the vertical fire test (UL 94), however, the addition of melamine was crucial for achieving the highest fire classification (UL 94-V0 rating). The presence of DP and Mel in the silica-epoxy nanocomposite promoted a large reduction (ranging from 53% up to 80%) in the heat release rate (HRR) and a delay (up to 31%) in the ignition time in the cone calorimetry experiments. Improved fire performance of the epoxy system was attributed to i) a condensed phase activity of silica, DP and melamine to form a protective thermal barrier during combustion and ii) a minor gas phase flame inhibition activity of DOPO component of DP. The mechanical characterization of the epoxy nanocomposites through tensile tests showed that the addition of DP increases the stiffness of the epoxy resin, resulting in a strong increase of Young modulus (up to 32%) and in a slight decrease of fracture strength, elongation at break and toughness. An increased glass transition temperature (up to 8%) of the epoxy system possibly due to hydrogen bonds and polar interactions of DP with the matrix was also observed.

1. Introduction

Epoxy resins are crosslinkable versatile polymers finding application in areas such as electronics, composites, coatings and adhesives. They are prized for their excellent physical, chemical, electrical and adhesive properties [1]. A wide range of epoxy resins with varying properties can be synthesized by reacting different epoxides with a variety of curing agents. Curing agents such as aromatic, aliphatic and cycloaliphatic amines are preferred for hardening epoxy resins due to their high reactivity and possibility for tuning curing kinetics, which can be adapted for various applications [1]. The use of aromatic curing agents offers good thermal stability and fire performance to the final product, although

they are toxic and subject of governmental restrictions [2]. An alternative is the use of aliphatic amines as curing agents. They are very reactive and enable quick curing of the epoxy resins at room temperatures albeit the final product has lower thermal stability. The use of cycloaliphatic curing agents offers a good balance between the aromatic and aliphatic curing agents as the resulting products have intermediate properties [3]. Like epoxy resins cured with aliphatic curing agents, the resins cured with cycloaliphatic curing agents are easily flammable and require the use of flame-retardant additives for fire safe applications. Halogenated flame-retardants have been commonly used in flame retardation of epoxy resins. However, the usage of some of these additives are regulated and banned because of their potential toxicity [4–7]. As

an alternative, development and use of silicone and phosphorus-based flame-retardants is considered as a viable option [8–12].

Epoxy resin with aliphatic components requires high levels of phosphorus (P) content (> 2 wt% P) to achieve satisfactory fire performance (UL 94-V0 classification) desired in many fire safe applications. A minimum 4 wt% P-content was needed when organic and inorganic phosphorus-based flame-retardants were used in glycerol and pentaerythritol based epoxy resins to achieve a V0 rating in UL 94 test. Similarly, a 5 wt% P (inorganic phosphorus flame-retardant) and 3 wt% P (organic reactive phosphorus flame-retardant) was needed to achieve a V0 rating for an aliphatic epoxy resin cured with a cycloaliphatic amine hardener [13]. In a recent work, synergistic combination of copper-decorated graphene together with ammonium polyphosphate (APP) has been used as flame-retardant for DGEBA based epoxy resin cured with an aliphatic amine. A minimum concentration of 28 wt% APP (> 5 wt% P) was required to achieve a V0 classification [14]. In another recent work, biobased based aliphatic epoxy resin containing phosphazene building block with 5 wt% P was developed to achieve V0 rating in UL 94 tests. A phosphorus silicone based novel flame-retardant polyhedral oligomeric silsesquioxane containing 9,10-dihydro-9-oxa-10-phosphaphenanthrene-10-oxide (DOPO-POSS) was developed for DGEBA based epoxy resin cured with aliphatic and aromatic curing agent. Higher concentration of DOPO-POSS (10 wt%) was needed to achieve a maximum fire performance (V1 rating) in case of epoxy resin cured with aliphatic amine [15].

Thus, it is clear that epoxy resins containing aliphatic components require higher concentration of phosphorus to achieve satisfactory fire performance and thus there is a need to develop more efficient green flame-retardant systems which can work at lower P loading. DOPO based phosphorus compounds are known for their effective in flame retardation of many polymers and non-toxic nature and thus can be considered an appropriate strategy to tackle above-mentioned challenges [11,16–19]. Recently, a non-toxic DOPO derivative, 6H-dibenz[c,e][1,2]oxaphosphorin,6-[(1-oxido-2,6,7-trioxa-1-phosphabicyclo[2.2.2]oct-4 yl)methoxy]-, 6-oxide, which will be indicated as "DP" throughout the paper, was synthesized using a green chemistry methodology [17] and applied in polyesters to achieve high level of fire protection. DP is considered as a hybrid flame retardant where the DOPO component with its gas phase activity is complemented by PEPA component which works in the condensed phase [17,20]. In an independent work a self-extinguishing behavior (UL 94-V0 rating) was achieved for DGEBA based epoxy resin containing 5.7 wt.% of DP and cured with an aromatic hardener [21]. The flame-retardant behavior of DP in epoxy resins containing aliphatic components is unknown and worthy of investigation.

In this work we have evaluated the flame-retardant performance of DP in DGEBA based epoxy resin cured with a cycloaliphatic curing agent and further developed strategies to improve its fire performance by incorporation of silica precursors and a nitrogen synergist. In-situ generated silica-epoxy materials were synthetized by using DGEBA resin and subsequently cured with aliphatic isophorone diamine as a cycloaliphatic hardener. DP as phosphorous-based flame-retardant additive was added, at two different P-loadings (i.e. 1 and 2 wt%) together with melamine as a nitrogen additive. The effect of P-N synergism on the flame retardancy of the silica-epoxy nanocomposites was investigated. Fourier-transform infrared spectroscopy with attenuated total reflectance (ATR-FTIR) was used to analyze the chemical composition consistency of the epoxy samples. The thermal and fire behaviors of the obtained nanocomposites were investigated in detail by means of thermogravimetric analysis (TGA), differential scanning calorimetry (DSC), pyrolysis combustion flow calorimeter (PCFC), cone calorimetry, UL 94 vertical flame spread tests, DIP-MS (direct insertion probe–mass spectrometry) and PY-GC-MS (pyrolysis–gas chromatography–mass spectrometry). Furthermore, the effect of various additives on mechanical behavior of the epoxy resin was investigated by tensile tests.
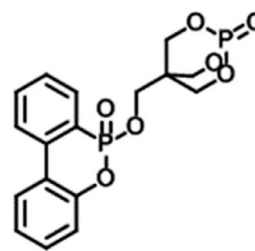

Fig. 1. Chemical structure of 6H-dibenz[c,e][1,2]oxaphosphorin,6-[(1-oxido-2,6,7-trioxa-1-phosphabicyclo[2.2.2]oct-4-yl)methoxy]-, 6-oxide (DP).

2. Materials and methods

2.1. Materials

Tetraethyl orthosilicate (TEOS, purity >99%), (3-aminopropyl)-triethoxysilane (APTS, purity >98%), anhydrous ethanol, 2,4,6-triamino-1,3,5-triazine (melamine, purity >99%) and 1,8-diazabicyclo(5.4.0)undec-7-ene (DBU, ACS grade) were purchased from Sigma-Aldrich (Switzerland) and used as received. A two-component epoxy resin (Hexion Specialty Chemicals GmbH, Germany), consisting of bisphenol A resin (Epikote[TM] Resin 827) and isophorone diamine (Epikure[TM] curing Agent 943, abbreviated as IPDA) was used to prepare nanocomposites. 6H-dibenz[c,e][1,2]oxaphosphorin,6-[(1-oxido-2,6,7-trioxa-1-phosphabicyclo[2.2.2]oct-4-yl)methoxy]-, 6-oxide (DP, Fig. 1) was synthesized by the procedure described in S1 of supporting information (SI) [17].

2.2. Preparation of in-situ silica-epoxy composites

The preparation of "in-situ" silica-epoxy composites was performed by the addition of APTS and TEOS (silica precursors) to a commercial epoxy resin system (DGEBA) and mixed properly preceding the addition of IPDA hardener, as reported in the literature [8,9,22,23]. Typically, mixtures of epoxy, DGEBA, and APTS with fixed weight ratio of epoxy: APTS were stirred for 2 h at 80 °C followed by addition of required quantity of TEOS, distilled water and ethanol to the silanized epoxy. Amount of both silica precursors was adjusted to get 2 wt% silica content in the epoxy samples. Then, the mixture was stirred vigorously for 90 min at 80 °C. The mixing vessel was then opened and kept for 30 min (at 80 °C) for ethanol and water removal. The temperature was then increased to 100°C and required quantity of DP was added to the mixture to achieve 1 and 2 wt% of P-content in the final mixture (Fig. 1). Subsequently, the reaction mixture was stirred for 60 min.

Table 1 summarizes the selected formulations together with their acronyms as well as the experimental P-content (P) in epoxy composites determined by ICP-OES analysis. To evaluate the effect of nitrogen (N_2) additive on fire performance of the epoxy composites, melamine was added to some samples as a N_2 source along with DP (~15.7 wt% of phosphorus content). Finally, the required quantity of hardener (IPDA) was added to the mixture at room temperature and mixed well for 5 min. The resulting mixtures were degassed under vacuum, in order to remove the residue amount of ethanol and water used in the sol–gel synthesis, poured into a steel mold, cured at 40 °C for 3 h), then post-cured at 150 °C for 2 h. Composites without silica were also prepared for comparison.

2.3. Characterization

Phosphorus content of the composites was measured using the inductively coupled plasma optical emission spectrometry method (ICP-OES), on a 5110 ICP-OES (Agilent Switzerland AG, Basel, Switzerland) apparatus. Sample preparation for ICP-OES consisted of mixing 100 mg of a sample with 3 mL HNO_3, followed by digestion using a microwave.

Table 1

Additives used in Epoxy (107.75 g) and hardener (26.8 g) to prepared FR-epoxy composites.

Sample	TEOS (g)	APTS (g)	EtOH (g)	H_2O (g)	DP (g)	Mel (g)	P (wt%)[a]
EPO	-	-	-	-	-	-	-
EPO_DP1P	-	-	-	-	18.2	-	1.60
EPO_DP2P	-	-	-	-	27.3	-	2.70
EPO_Mel	-	-	-	-	-	9.1	-
EPO_DP2P_Mel	-	-	-	-	27.3	9.1	2.60
EPO2Si	6.92	3.61	0.85	2.75	-	-	-
EPO2Si_DP2P	6.92	3.61	0.85	2.75	27.3	-	2.20
EPO2Si_Mel	6.92	3.61	0.85	2.75	-	9.1	-
EPO2Si_DP1P_Mel	6.92	3.61	0.85	2.75	18.2	6.1	1.56
EPO2Si_DP2P_Mel	6.92	3.61	0.85	2.75	27.3	9.1	2.42

[a] Phosphorus (P) content (wt.%) in the composites was determined by ICP-OES analysis.

ATR-FTIR spectra of samples were recorded using a Bruker Tensor 27 FTIR spectrometer (Bruker Optics, Ettlingen, Germany), equipped with a single reflection attenuated total reflectance (ATR) accessory with 4 cm^{-1} resolution and OPUS[TM] 7.2 software was used for data analysis.

The flammability of epoxy composites was assessed by UL 94-VB vertical burning tests prescribed by IEC 60695-11-10 using a sample size of 13 × 125 x approx. 3 mm^3. Simultaneously, an Flir A40 IR Camera (FLIR Systems Inc., Wilsonville, USA) equipped with UL 94-VB apparatus was used to monitor the flame propagation during the burning tests. For each sample, the IR video was recorded (ThermaCAM Researcher Professional 2.10, FLIR Systems Inc., Wilsonville, USA) to observe the temperature profile that highlights 3 main steps occurring with flame propagation [24,25]. Recording was started once the flame was removed from the sample and was stopped after the flame was extinguished or reached the sample holder.

Thermogravimetric analysis (TGA) was performed on under N_2 and air (gas flow of 50 mL/min) using a NETZSCH TG 209 F1 instrument (NETZSCH-Gerätebau GmbH, Selb, Germany). All the analyses were carried out from 25 to 800 °C at a ramp of 10 °C/min.

Differential scanning calorimetry (DSC) analyses were carried out in a DSC 214 Polyma instrument (NETZSCH-Gerätebau GmbH, Selb, Germany) in a two repeating cycles from 20 to 300 °C at a ramp of 10 °C/min, under a N_2 flow of 50 mL/min. The onset values in the second heating cycle were used for the evaluation of glass transition temperatures (T_g) through the "tangent method". The completeness of curing was confirmed by looking at the absence of any exothermic peak in the first heating cycle.

Cone calorimetry test was carried out on a horizontally placed specimen (100 × 100 × 3 mm^3) without any grids following the ISO 5660 standard. Cone calorimeter from Fire Testing Technology, East Grinstead, London, UK was used with an irradiative heat flux of 35 kW/m^2 Test was useful to determine heat release rate (HRR), peak of heat release rate (pHRR), average specific extinction area (SEA), total smoke release (TSR), total heat release (THR) and the final residue.

Heat release rates (HRR) was also determined following ASTM D7309 using pyrolysis combustion flow calorimeter (PCFC) (Fire Testing Technology Instrument, London, UK). Composite samples (~7 mg) were heated from 150 to 750 °C at a rate of 1 °C/s in the pyrolysis zone.

Pyrolysis-Gas Chromatography Mass Spectrometry (Py-GC–MS) measurements were performed by placing about 30–100 μg of sample in a quartz tube (1 mm internal diameter x 25 mm length). The sample was then loaded in the pyrolysis probe (Type 5200, CDS Analytical, Inc., Oxford, PA, USA) and placed in the special inlet at the interface. The sample was pyrolyzed under inert atmosphere for 30 s (helium, 800 °C). The volatiles were passed through a Hewlett-Packard 5890 Series II gas chromatograph for separation and then molecules were analyzed by a Hewlett-Packard 5989 Series mass spectrometer.

Direct inlet probe mass spectroscopic (DIP-MS) measurements were carried out using a Finnigan/Thermoquest GCQ ion trap mass spectrometer (Austin, TX, USA) equipped with a DIP module. **DIP-MS** was useful to detect possible volatile products. Nearly 1 mg of composite sample taken in a quartz cup located at the tip of the probe was inserted into the ionization chamber. Measurements were performed at an ionization voltage of 70 eV, temperature of the ionic source of 200 °C, <10^{-6} mbar pressure and probe temperature ramp 60 °C/min from 30 to 450 °C.

Energy dispersive X-ray spectra (EDX) were recorded using a Hitachi S-4800 scanning electron microscope (Tokyo, Japan) equipped with Inca X-sight device from Oxford Instruments (Tokyo, Japan). During EDX measurements, acceleration was maintained at 20 kV and with emission current of 15 mA at a working distance of 15 mm.

Tensile tests were performed using specimen as per ASTM standard TYPE 1 dimensions. According to ASTM D638 with a Zwick/Roell Z100 (Zwick/Roell, Ulm, Germany) testing machine. The crosshead speed was 5 mm/min. All results are an average of nine measurements.

3. Results and discussion

3.1. Chemical characterization of the in-situ silica-epoxy composites

ATR-FTIR spectra of composite samples prepared in this work are shown in Fig. S1. The main differences between the sample containing melamine and DP with a P-loading equal to 2 wt% and cured (**EPO**) and uncured (**EPO_WH**) pristine epoxy are explained. It is worth noticing that the well-defined and intense characteristics bands of the epoxy functional groups at 970 cm^{-1}, 912 cm^{-1} and 870 cm^{-1} in **EPO_WH** disappeared in cured samples, confirming the completeness of curing process. Additionally, the absorption bands between 1050 cm^{-1} and 1150 cm^{-1} in **EPO2Si** suggest the formation of the silica phase from APTS and TEOS (silica precursors) through the well-established sol–gel reactions [9]. The incorporation of DP into the in-situ silica-epoxy system resulted in the appearance of new characteristic bands. In particular, the weak shoulder at 970 cm^{-1} can be attributed to the existence of P–O–C bonds [26], while the intense band near 1020 cm^{-1} indicates the presence of ortho-disubstituted benzene derivatives [27,28]. The band around 760 cm^{-1} can be attributed to the P-C stretching vibration and the band at 1140 cm^{-1} to P=O stretching [29–32], due to the presence of PEPA (1-(oxo-4-hydroxymethyl-2,6,7-trioxa-l-phosphabicyclo[2.2.2]octane)) unit in DP structure (Fig. S1). The bands located between 2860 cm^{-1} and 2970 cm^{-1} can be attributed to the stretching vibration of the C–H and the band at 800 cm^{-1} refers to the bending vibration of the N–H bond, presents in the cured epoxy and melamine [33–35]. The ATR-FTIR spectra are, therefore, consistent with the chemical composition of composites.

3.2. Thermal analysis

In Fig. 2 DSC thermograms of pristine epoxy and epoxy composites are shown. The glass transition temperature (T_g) was estimated as the extrapolated onset temperature from the second heating up curve. The completeness of the curing reaction was verified from the first heating
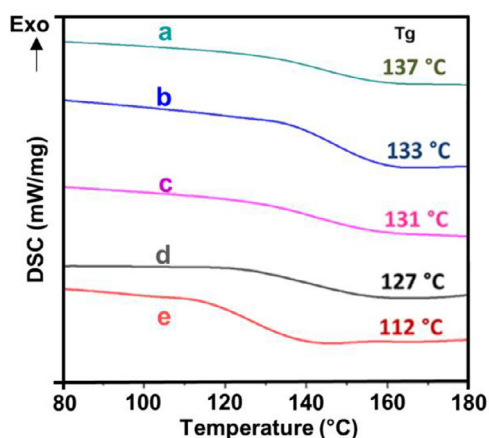
Fig. 2. DSC thermograms (second heating cycle) of **EPO2Si_DP1P_Mel** (a), **EPO_DP2P** (b), **EPO2Si_DP2P_Mel** (c), **EPO** (d), **EPO2Si** (e).

cycle through the absence of any residual exothermic peak. The glass transition temperature was determined by using the "tangent method", following the procedure reported in Section 2.3. A significant reduction in the T_g of the composites containing silica alone (Fig. 2) highlights the negative influence of the hybrid co-continuous network of silica on epoxy chains mobility [9,36].

It is noteworthy that, the incorporation of DP (2 wt% P) to the in-situ silica-epoxy network increases the T_g of the cured resins. The stiffness effect of DP on the polymer chains is likely due to the formation of hydrogen bonds between the oxygen of DP structure (Figs. 1 and S2) and hydroxyl groups formed because of the cross-linking process [17,37]. In addition, polar moieties of DP (i.e., PEPA groups) can interact with the epoxy groups of DGEBA chains to assure compatibility, contributing to enhance the rigidity of the epoxy system [37]. Besides, melamine is a trimer of cyanamide and it was demonstrated to form hydrogen bonded network with imide units in blends of the styrene/maleimide copolymers. These interactions resulted in T_g increase of the copolymer, as this H-bonds crosslinking restricts the motion of polystyrene segments [38]. The establishment of hydrogen bond interactions between the oxygen of DP and melamine may explain the increase in the T_g (up to ~23%) in case of **EPO2Si_DP1P_Mel** with respect to **EPO** and **EPO2Si** samples [37,38].

Figs. 3 and 4 show the TGA curves of all studied systems recorded in N_2 and air atmosphere respectively. The thermal degradation mechanism of pristine epoxy cured with IPDA is reported in the literature [39,40]. In N_2 atmosphere, particularly, some principal volatile products are formed at about 280 °C, specifically acrolein, acetone and allyl alcohol. High molecular weight products along with more complex phenolic compounds evolve during the main decomposition step of the cross-linked resin (beyond 340 °C) [40]. In an inert atmosphere, no weight changes were observed between 400 and 600 °C, because of the formation of a very stable aromatic char. As reported in the literature [40,41], in air, O_2 leads to the formation of several oxidized species like ketones, amides and a combination of aromatic or/and aliphatic aldehydes, which are almost completely oxidized at higher temperatures (400–600 °C). In N_2 atmosphere (Fig. 3), the blank epoxy decomposes via one main decomposition step around 350 °C. The behavior in air appears to be different, showing two main degradation steps around 350 °C and 500 °C, in agreement with the degradation pathways of an aliphatic epoxy resin [40,41]. Besides, the incorporation of melamine in some samples leads to the appearance of a third degradation step below 300 °C (in air), possibly due to its decomposition of melamine to ammonia and subsequently to N_2 in presence of O_2 [42]. As it can be seen in Fig. 3(a, c) and Fig. 4(a, c), the addition of DP with or without melamine results in an earlier thermal degradation of the resins compared to **EPO**

and **EPO2Si**. This early stage decomposition may be mainly ascribed to the formation of acidic phosphorus species during the degradation of DP and the production of non-flammable volatiles (P-species and N_2) [43,44] together with a minor effect due to the acidic characteristics of the in-situ sol-gel silica [45], which accelerate the decomposition of the composite [46].

The presence of DP strongly increases the thermal stability of the composites and forms a stable aromatic char at high temperatures [47]. This finding is supported by the lowering of mass loss in air and N_2 atmosphere in the first step (< 400 °C) and second step (400–600 °C). The increase in the residues of DP-containing nanocomposites in air and N_2 (Table S1) supports the argument of stable char formation [47]. DP decomposes to phosphoric acids responsible for dehydration reactions with the epoxy resin. Besides, DP decomposes to PEPA units that can also produce phosphoric acids during the carbonization process [17,48]. This secondary effect due to the PEPA's condensed phase activity may contribute strongly to boost the char formation. The effect of DP on the thermo-oxidative stability of the composites results in a remarkable increase in the residue of **EPO_DP2P** (13%) compared to **EPO** (0.7%) at 800 °C. The lowering of $T_{5\%}$ in the case of **EPO2Si_DP2P** compared to the **EPO** can be ascribed to the acidic characteristics of the in-situ sol-gel silica and the formation of acidic phosphorus species, which promote stable char formation through dehydration reactions [9,46-49].

3.3. Fire behavior of the in-situ generated silica-epoxy materials

Epoxy composites along with pristine **EPO** were subjected to vertical flame spread tests to assess their flammability. **EPO, EPO_DP1P, EPO2Si, EPO2Si_Mel** and **EPO_Mel** samples could not be classified (Table 2) although the presence of silica nanoparticles (**EPO2Si**, Fig. S3b) guaranteed the formation of a coherent char during the fire test. It is worth pointing out that for all investigated compositions, the presence of DP with or without silica nanoparticles in the polymer matrix prevents dripping phenomena (Table 2), due to the increase of the melt viscosity of the burning system [9,50]. Therefore, the addition of DP or silica nanoparticles to the epoxy resin was crucial for obtaining a non-dripping classification. This suggests that DP and silica nanoparticles can act via a condensed phase activity [9,17]. Sample containing DP (2 wt.% P, **EPO_DP2P**) burned only partly, producing a very coherent and abundant char (Fig. S3c) during the first flame application. This protective layer of coherent char allowed a strong decrease of the t_2 extinguishing afterflame time, which additionally supports a predominant condensed phase activity of DP and this sample achieved UL 94-V1 classification. When DP (2 wt% P) and silica nanoparticles are both present in the epoxy resin (**EPO2Si_DP2P**) the first flame application was followed by a delay of t_1 afterflame time with respect to **EPO_DP2P**: this indicates that silica nanoparticles influence the char-forming mechanism in agreement with TGA results. Thus, in the presence of silica nanoparticles the resulting char showed higher efficiency, acting as oxygen barrier and mostly as thermal shield [9], hence inducing self-extinguishing capacity to the epoxy sample at the second flame application although any classification could be attributed.

Besides, a comparison of the after flame times (t_1 and t_2) of **EPO_DP2P** and **EPO_DP2P_Mel** reveals that melamine decomposition to N_2-based volatiles allows boosting of fire retardant behavior through a dilution effect of flammable gases, leading to a decrease of the t_1 extinguishing time (Table 2). The addition of DP (2 wt% P) in combination with melamine and silica nanoparticles to the epoxy resin was crucial to obtain a non-dripping "UL 94-V0" classification. **EPO2Si_DP2P_Mel** shows self-extinguishing through a synergistic effect of dilution in the flame zone and thermal barrier due to a combined condensed phase activity of DP and silica nanoparticles during the combustion process. Conversely, it is worthy to note that samples containing lower concentration of DP (i.e. 1 wt% P) could not achieve any classification in the UL 94-VB test, even in the presence of melamine and silica.

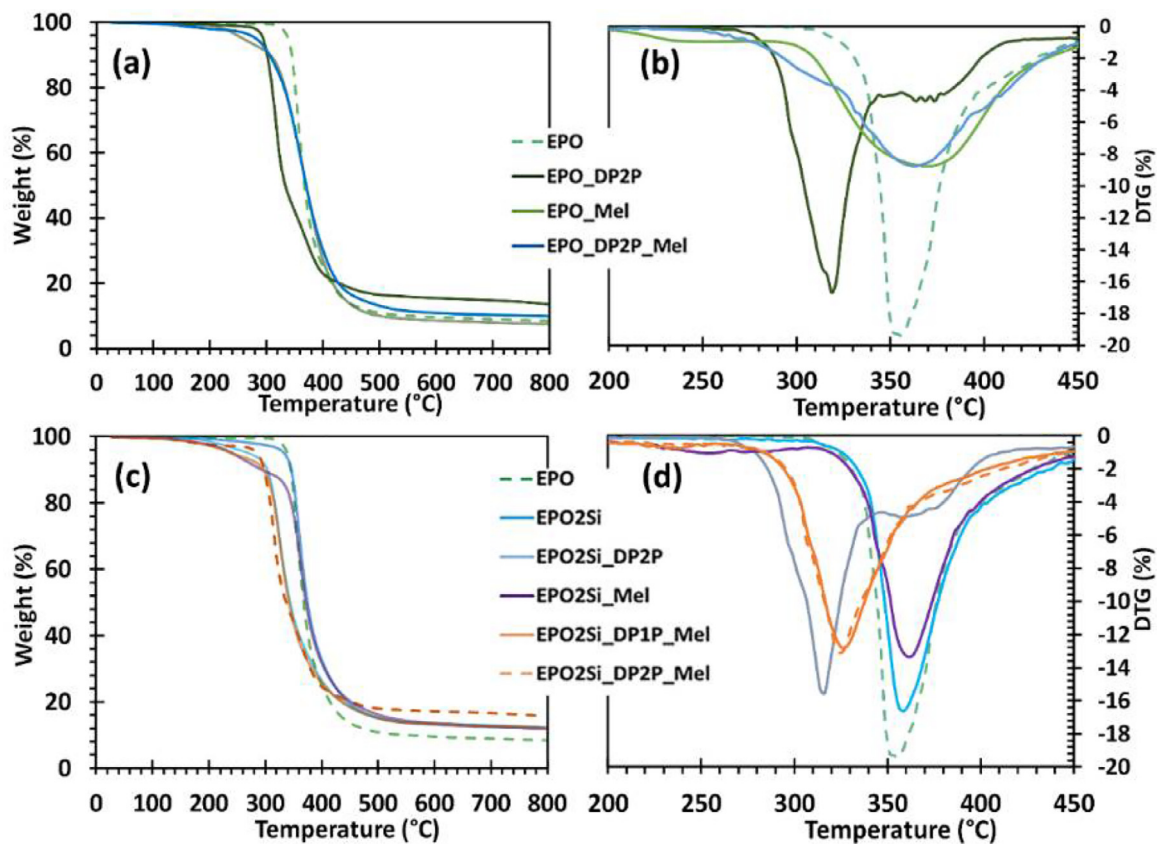**Fig. 3.** TG (a–c) and DTG (b–d) curves of pristine epoxy (**EPO**) and epoxy composites measured under inert (N$_2$) atmosphere.
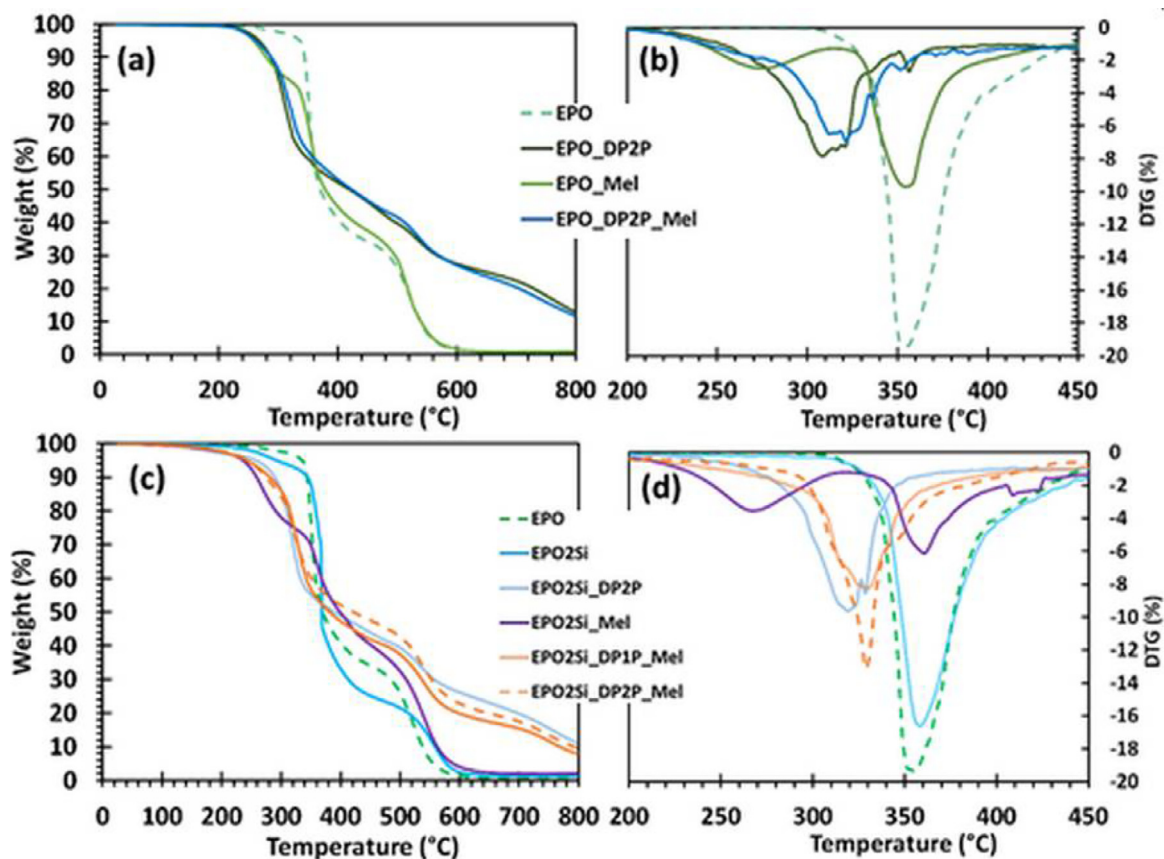

**Fig. 4.** TG (a–c) and DTG (b–d) analysis of pristine epoxy (**EPO**) and epoxy composites under air.

Table 2
Results of flame spread tests in vertical configuration.

Sample	UL 94 Class	Dripping	t_1 in sec.[2]					t_2 in sec.[3]				
EPO	NC[1]	Yes						-				
EPO_DP1P	NC	No						-				
EPO_DP2P	V1	No	23	20	24	18	25	*1*	*3*	*1*	*5*	*2*
EPO_Mel	NC	Yes						-				
EPO_DP2P_Mel	V1	No	17	18	16	19	15	*2*	*3*	*2*	*3*	*1*
EPO2Si	NC	No						-				
EPO2Si_DP2P	NC	No	31	33	31	32	34	*0*	*0*	*0*	*0*	*0*
EPO2Si_Mel	NC	No						-				
EPO2Si_DP2P_Mel	V0	No	0	0	0	0	0	*5*	*3*	*5*	*2*	*4*
EPO2Si_DP1P_Mel	NC	No						-				

[1] **NC**: not classified.

[2] t_1 = Duration of flaming after first flame application.

[3] t_2 = Duration of flaming after second flame application.
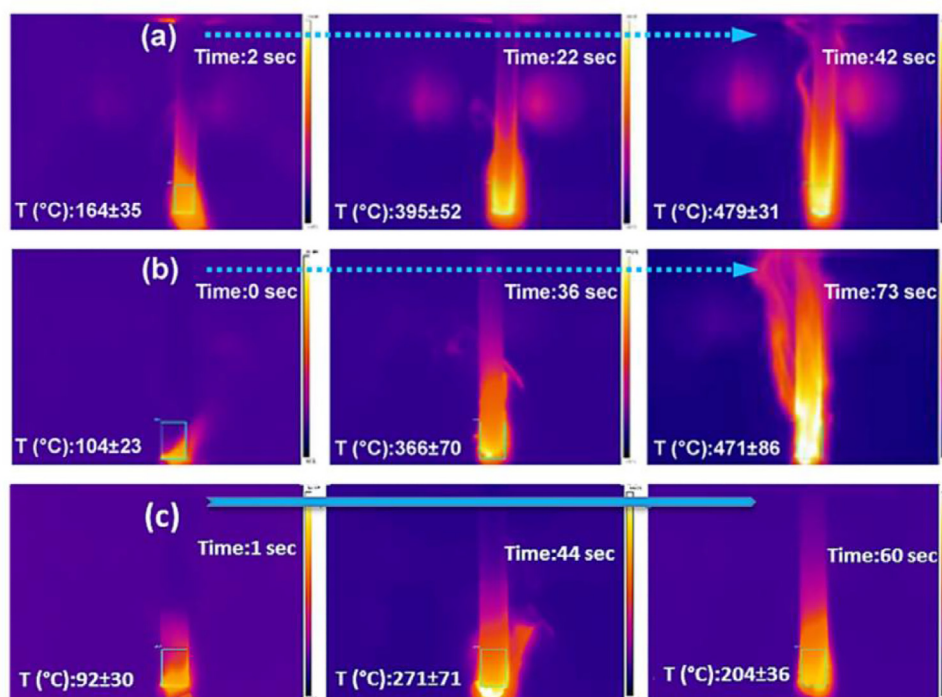
Fig. 5. IR camera images showing flame profiles and temperatures at "contact", "middle" and "end" phases for (a) **EPO**, (b) **EPO2Si** and (c) **EPO2Si_DP2P_Mel**.

Fig. 5 shows the burning behavior of composites recorded by an IR-camera during UL 94 vertical burning test. In detail, three main steps can be identified for the burning process of **EPO** and **EPO2Si** samples:

(I) *Contact phase:* material captures the flame followed by rapid rise of the surface temperature.

(II) *Middle flame phase:* consumption of the burning material occurs along with the advancing flame front; subsequent increase in temperature, and volatiles production, which feed the flame in the gas phase.

(III) *End flame phase:* tipping point for the combustion process is achieved; flame engulfs the sample and reaches the holding clamp.

The temperatures at the three main steps for **EPO** and **EPO2Si** were taken at the end of the flame contact phase, when the flame reaches the middle of the sample and when the flame envelopes the sample reaching the holding clamp. Fig. 5b shows that the presence of 2 wt% silica affects the fire behavior, leading to lower temperatures and delayed flame propagation. As can be seen, the addition of DP and melamine into silica-epoxy nanocomposite (**EPO2Si_DP2P_Mel**) strongly influences the fire performances, resulting in a very limited flame propagation and rapid extinguishment once the flame is removed. As previously mentioned, the combination of DP, silica nanoparticles and melamine in the epoxy

resin assure instantaneous self-extinction through the occurrence of a synergistic effect. Thus, flame propagation stops immediately, leading to a cooling effect during the burning process (Fig. 5c). The endothermic decomposition of DP [11,51] and melamine [46,47,49], in combination with an increased thermal stability due to the presence of DP with or without silica nanoparticles results in ~40% reduction in the surface temperatures during the contact and middle flame phases compared to **EPO** and **EPO2Si** (Fig. 5b,c). The cooling effect is relevant in the case of the end flame phase where the presence of a very stable and abundant char (Fig. 5c and Fig. S3d) chiefly acting as thermal shield leads to a remarkable temperature reduction (~60%) with respect to **EPO** and **EPO2Si** (Fig. 5b,c).

In agreement with UL 94 vertical burning test results, fire performance of epoxy nano composites were evaluated by PCFC measurements (Fig. 6). The addition of DP in the epoxy resin has a strong effect in reducing the HRC (Heat Release Capacity) and THR (Total Heat Release) of the epoxy resin, confirming its efficacy as a flame-retardant (Table S2). However, it has a notable effect on the residue, highlighting its strong condensed phase activity [11,42,51]. It is noteworthy that, the addition of DP (**EPO_DP2P**) in the epoxy resin is essential for a strong reduction (~32%) in the pHRR (peak Heat Release Rate, Table S2). Narrow and sharp heat release peak in the HRR curves of **EPO, EPO2Si,**

Table 3
Results from cone calorimetry tests for the investigated samples.

Sample	TTI (s)	TTF (s)	THR (MJ/m^2)	MLR (g/s•m^2)	HRR (kW/m^2)	pHRR (kW/m^2)	Residue (wt.%)
EPO	38±3	117±2	96±2	77±3	532±22	2550±368	1±0.7
EPO_DP2P	31±1	346±1	61±5	19±3	135±18	744±75	16±0.6
EPO_DP2P_Mel	50±5	406±3	62±7	17±2	158±11	730±128	13±0.5
EPO2Si	40±6	130±4	79±10	42±3	412±10	1964±81	4±0.5
EPO2Si_DP2P	28±4	512±3	68±9	13±5	106±8	516±111	12±0.7
EPO2Si_DP2P_Mel	42±5	172±5	57±5	33±2	247±11	909±121	10±0.6
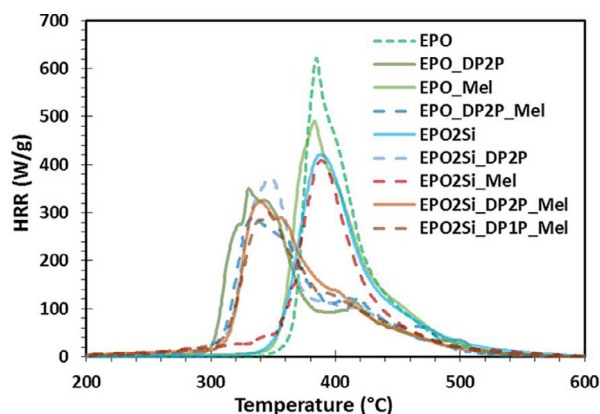
Fig. 6. HRR (Heat Release Rate) curves vs. temperature for all the investigated samples measured using PCFC.
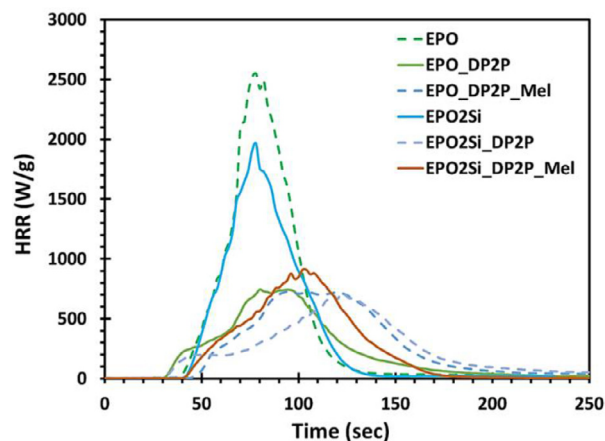
Fig. 7. Heat release rate (HRR) observed in pristine epoxy (**EPO**) and epoxy composites measured using cone calorimeter.

EPO_Mel and **EPO2Si_Mel** is observed, because of a large amount of heat released in a short time. Conversely, the HRR curves of **EPO_DP2P, EPO2Si_DP2P, EPO_DP2P_Mel** and **EPO2Si_DP2P_Mel** show a broad and flattened profile, indicatingthe heat release is spread over a longer time scale. The incorporation of DP results in a catalyzed thermal decomposition, possibly due to the formation of acidic phosphorus species, and in lower temperatures at which pHRR appears (Fig. 6). DP actively promotes the char formation at an early stage via dehydration reactions [52], favoring the formation of a thermal protective barrier [9]. The addition of DP, with a phosphorous concentration equal to ∼2 wt%, melamine and silica nanoparticles in the epoxy resin can effectively prevent further combustion, allowing the sample to achieve a UL 94-V0 classification.

EPO_DP2P_Mel shows a lower residue compared to **EPO_DP2P**; however, the lowering of the residue caused by melamine is negated by the addition of silica nanoparticles (**EPO2Si_DP2P_Mel**) [53–55]. The N$_2$-based compound (i.e. melamine) when added to the epoxy resin, led to an increase in the heat release capacity (**EPO_Mel**). It can be due to the exothermic oxidation of ammonia [44,45]. A comparison between the residues of **EPO_Mel** and **EPO2Si_Mel** after the PCFC experiments further highlights the barrier effect of silica nanoparticles during the char-forming process.

In order to investigate the combustion behavior, pure epoxy resin and in-situ silica-epoxy composites were exposed to a constant heat flux in the cone calorimeter (ISO 5660 standard). It is noteworthy pointing out that, DP-containing samples show a remarkable reduction of HRR (53-80%), MLR (Mass Loss Rate) and THR (Total Heat Release) with or without melamine (Table 3), though the presence of silica alone already promotes a significant decrease of the aforementioned parameters for these systems, respectively 22%, 45% and 18%. In comparison to the virgin epoxy resin (**EPO**) the strong increase in residue for DP containing samples is in agreement with the hypothesis that DP acts strongly in the condensed phase, where the formation of a stable and abundant char leads to an incomplete combustion and a lower amount of combustible gases supplied from the polymer bulk [9,17]. DP exhibits a gas phase activity, as revealed by a slight increase of CO/CO$_2$ ratio (Table 4). The phosphorous species formed in the gas phase act through a flame inhibition, suppressing the radical overshoot in flame and chain reactions of the oxidation of hydrocarbons in the gas phase, thus diminishing the heat release [52].

Cone calorimetry data are in agreement with the PCFC results, the addition of DP broadens the HRR curves (Fig. 7). In addition, melamine degradation leads to the formation of N$_2$, increasing the time to pHRR and delaying the time to ignition ∼31% through dilution of combustible gases (Fig. 7 and Table 3) [42,51]. The incorporation of DP into silica-epoxy nanocomposite (**EPO2Si_DP2P**) results in the lowest TTI (Table 3), due to the acidic characteristics of sol-gel silica, leading to an earlier thermal degradation of the resin (Section 3.2). In addition, **EPO2Si_DP2P** shows a significant increase in the time to pHRR (Fig. 7), together with a remarkable reduction in HRR (∼80%) and pHRR (Table 3). These effects on the latter cone parameters and the increase in the residues at the end of the cone calorimetry tests (Table 3) confirm that the combination of DP, silica nanoparticles and melamine can boost the condensed phase activity (Section 3.2), because of the formation of relevant amount of char, which strongly influences the heat transfer phenomena during the combustion process [9].

Fig. S4 clearly shows that in comparison to the virgin epoxy resin (**EPO**) the volume of residue increases in presence of silica (**EPO2Si**), DP (**EPO_DP2P**) and melamine (**EPO_DP2P_Mel**) in the matrix. In particular, when the latter additives are combined in the matrix, intumescence was observed (Fig. S4d and f) [49,56]. Fig. S4 also shows the presence of thin white ceramic-like silica layer on the char residues of **EPO2Si** (Fig. S4b), **EPO2Si_DP2P** (Fig. S4e), and **EPO2Si_DP2P_Mel** (Fig. S4f and S7), further supports the role of silica in the char-forming mechanism [54,55]. The addition of DP has a detrimental effect in the smoke production (Table 4). In fact, SEA (Smoke Extension Area), TSR (Total Smoke Release), CO/CO$_2$ yields increase; this behavior is typical for materials with a flame-retardant activity in the gas phase [57].

Table 4
Smoke parameters from cone calorimetry tests for the investigated samples.

Sample	TSR (m^2/m^2)	SEA (m^2/kg)	CO yield (kg/kg)	CO_2 yield (kg/kg)	CO/CO_2
EPO	1840±206	131±35	0.03±0.003	0.4±0.1	0.06
EPO_DP2P	2660±278	337±34	0.06±0.0004	0.7±0.1	0.08
EPO_DP2P_Mel	2660±211	338±26	0.05±0.002	0.6±0.03	0.08
EPO2Si	1981±266	241±35	0.03±0.004	0.7±0.02	0.04
EPO2Si_DP2P	2721±312	201±81	0.04± 0.004	0.3± 0.2	0.1
EPO2Si_DP2P_Mel	2577±281	325±4	0.05±0.002	0.5±0.02	0.08
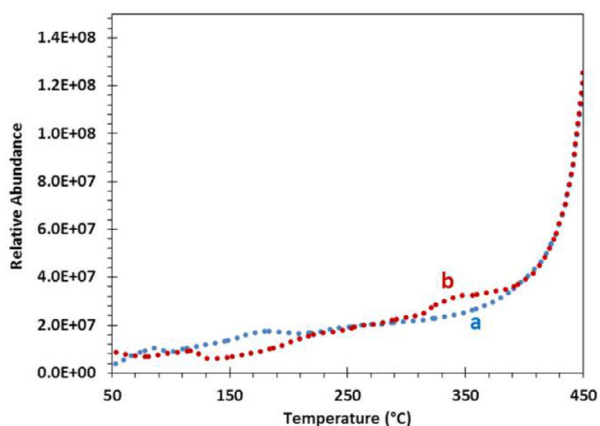
Fig. 8. DIP-MS total ion thermograms of **EPO** (a) and **EPO2Si_DP2P_Mel** (b).

Fig. 9. ATR-FTIR spectra for residual chars obtained after the vertical burning test of **EPO** and **EPO2Si_DP2P_Mel**.

3.4. Evolved gas analysis

The decomposition mechanism of composites and the influence of the various additives on the released gases was investigated in detail by PY-GC-MS and DIP-MS analyses. As already reported for similar systems [39,58], the following most abundant compounds were identified: bisphenol A, 4,4′-(cyclopropane-1,1-diyl)diphenol, 4-isopropylphenol, 4-isopropenylphenol, phenol, benzene, naphthalene, toluene, 2-methylpent-2-en-1-ol, 3-hydroxy-2-methylpentanal, o-cresol, 2-ethylphenol, and 2-allyl-4-methylphenol along with several other aromatic products in very low amounts. One of the main decomposition products of DOPO, dibenzofuran, was also detected for **EPO2Si_DP2P_Mel** [59].

Fig. 8 shows total ion thermograms of **EPO** and **EPO2Si_DP2P_Mel** obtained through DIP–MS analysis, which additionally confirmed the formation of many decomposition products (Fig. 8). **EPO** and **EPO2Si_DP2P_Mel** release approximately the same amount of decomposed volatile species with increasing temperature up to 450 ˚C (Fig. 8). As reported in Table S3, the outcome of DIP-MS data for **EPO2Si_DP2P_Mel** suggests at this temperature range (200–450 ˚C) the production of some major species. The presence of these compounds was also observed for DP, although in a different polymer matrix (i.e. polyester) [17]. According to the DIP-MS results (Table S3), the P-O bond of DP breaks and phosphorus species are released [17]. In Fig. S5 the thermograms of each species formed from the decomposition of DP are shown.

As reported in the literature, the decomposition pathway for epoxy resins in an inert atmosphere and at high temperature begins with the elimination of water from the secondary alcohol group and concludes with the dominant formation of bisphenol A, 4,4′-(cyclopropane-1,1-diyl)diphenol, 4-isopropylphenol, 4-isopropenylphenol and phenol [39,52,58]. The analysis of DIP-MS data for **EPO** (Fig. S6), confirmed the formation of major decomposition products of pristine epoxy resin summarized in Table S4; the m/z ratio used for their detection are also listed in the same table. The same species were also observed in the PY-GC-MS measurements. Therefore, the experimental results are con-
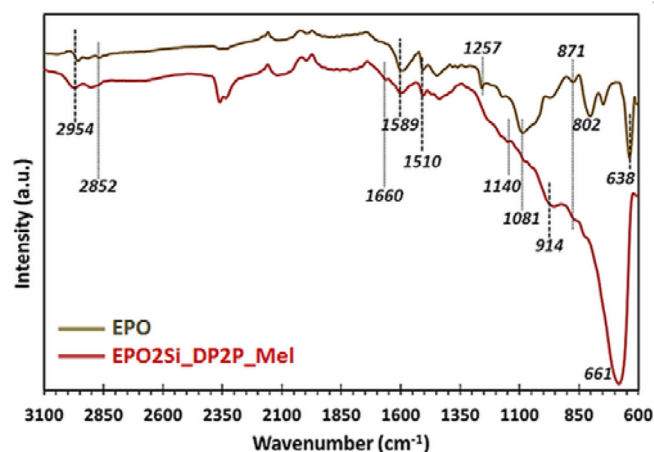
sistent with the mechanism reported in the literature summarized above [39,52,58].

3.5. Residue analysis

In UL 94, cone calorimetry, PCFC and TGA experiments significantly higher residue were observed for DP containing samples. To investigate the action of DP in the condensed phase, elemental analysis of the residue remaining after the UL test was performed. The concentration and ratio of elements can indicate their possible condensed phase contributions. Table S5 summarizes the Energy-Dispersive X-ray analysis (EDX) of the char residue of **EPO, EPO2Si, EPO_DP2P, EPO_DP2P_Mel, EPO2Si_DP2P** and **EPO2Si_DP2P_Mel** obtained after the vertical burning test. As expected, elements C, N, O were observed for all residue and Si and P were observed when silica and DP were present in the matrix. The retention of Si element after combustion is consistent with the earlier discussed role exerted by silica in the condensed phase (Table S5). A significantly higher P retention in the residue is observed for DP containing samples. For example, in **EPO_DP2P** a higher P-content (4.5 wt%, Table S5) is observed in its residue (UL 94 vertical spread test) compared to the initial P-content (2.7 wt%, Table 1) of the sample. Similarly, other DP containing samples **EPO_DP2P_Mel, EPO2Si_DP2P, EPO2Si_DP2P_Mel** also exhibit higher P-content (Table S5) in their respective residues compared to their initial P-content (Table 1). Increased P-content in the char residue after UL 94 vertical spread tests clearly confirms condensed phase activity of DP. In addition, presence of melamine catalyzes higher P-content in the residue (**EPO_DP2P_Mel**- 10.4 wt%, **EPO2Si_DP2P_Mel**- 8.6 wt%) which clearly indicates their condensed phase interaction.

ATR-FTIR analysis (Fig. 9) was performed to qualitatively study the chemical composition of the residual chars produced in the vertical flame spread test of **EPO** and **EPO2Si_DP2P_Mel**. The peak around 638 cm^{-1}, 802 cm^{-1} and 871 cm^{-1} for char formed from pristine epoxy polymer confirms the presence of aromatic C–H stretching in meta, para and ortho, respectively [41,60]. The combustion products of DGEBA

epoxy resin contain alkoxy C–O and phenol C–O groups with stretching bands at 1081 cm^{-1} and around 1257 cm^{-1}, respectively [41]. The bonds between the carbons of the aromatic ring result in a stretching vibration at 1510 cm^{-1} [35,61]. The presence of the bands at 2852 cm^{-1} and 2954 cm^{-1} may be due to the stretching vibrations of the C–H, while the broad band at 1589 cm^{-1} can be assigned to N–H stretching vibration of the secondary amine formed during cross-linking reactions [34]. The ATR-FTIR spectrum analysis of **EPO2Si_DP2P_Mel** char shows broad peaks at 661 cm^{-1} and 914 cm^{-1}, which may be ascribed to stretching vibrations of P–C and P–O respectively [26,35]. The high intensity of 661 cm^{-1} and 914 cm^{-1} peaks reveals the production of a noticeable amount of pyrophosphates and polyphosphates. The band at 1108 cm^{-1} may be attributed to stretching vibration of silica units [62], well known for the shielding effect [9]. The presence of P–N stretching vibrations in the char causes the appearance of the band around 1430 cm^{-1}, which supports a condensed phase interaction between DP and melamine during the combustion [35].

In agreement with TGA and cone calorimetry results, the presence of C=C stretching band around 1589 cm^{-1} supports the occurrence of the carbonization process due to dehydration reactions between acid phosphorous compounds (i.e. polyphosphoric acids, phosphorus oxynitride) and epoxy resin, promoting char formation [46,47,49,60]. Also, the band at 1140 cm^{-1} may be attributed to P=O stretching [29–32], mainly due to the condensed phase activity of PEPA, which produces phosphoric acid compounds [17,48]. This finding is also in agreement with the strong increase of char residue observed in presence of DP in previously reported results [35]. The combustion process produces low molecular weight oxidized species which are responsible for a band around 1660 cm^{-1}, which is usually attributed to the C=O stretching [40,41]. Therefore, as suggested by char residue analysis of **EPO2Si_DP2P_Mel** (Table S5), the ATR-FTIR results support a weighty condensed phase action of DP (Fig. 9).

3.6. Proposed flame-retardant mechanism

In view of the residue analysis and evolved gas analysis, fire-retardant action of DP in the gas and condensed phases was hypothesized. It is worth mentioning that, the relative abundances of the main volatile compounds (bisphenol A, 4,4′-(cyclopropane-1,1-diyl)diphenol, 4-isopropylphenol, 4-isopropenylphenol, phenol) as a function of temperature released from **EPO** (Fig. S6) are lower compared to the amount of phosphorous species produced by the decomposition of DP in the temperature range from 200 to 450 °C (Fig. S5 and Fig. S6). DIP-MS analysis confirmed the formation of major fragments represented by DOPO radical (m/z 215) and benzofuran (m/z 168) in the case of **EPO2Si_DP2P_Mel**. The presence of benzofuran supports the occurrence of the decomposition pathway of DOPO radical, through the production of $PO^{\bullet}$ (m/z 47) (Table S3) [17,57]. It is well known that, in air, $PO^{\bullet}$ radicals can act in the gas phase and suppressing the active $H^{\bullet}$ and $OH^{\bullet}$ in a flame [52,63]. Thus, the gas phase activity of the flame-retardant suggested by the cone calorimetry results may be due to the $PO^{\bullet}$ formed during the pyrolysis process.

As reported in the literature [40,41], absence of a flame inhibition mechanism would allow the normal yield of the active $H^{\bullet}$ and $OH^{\bullet}$ species, leading to the production of several of low molecular weight oxygenated species. To highlight the role of DP in the molecular reactions of **EPO** degradation process (in inert atmosphere) at elevated temperatures in air and based on the results discussed so far, a general decomposition mechanism of DP relevant in flame retardation process is proposed (Scheme S1). It is well known that, oxygen may act by extracting a $H^{\bullet}$ from the major decomposition products of epoxy resin to form $HO_2^{\bullet}$ and later turned into $OH^{\bullet}$ active oxygen species [52,57,64]. However, DOPO radicals (species R and S of Table S3, Scheme S1) may convert into volatile phosphorus species such as $PO^{\bullet}$, $PO_2^{\bullet}$ and $HOPO_2^{\bullet}$ (flame suppressors) neutralizing the active oxygen radicals [52]. This second effect may strongly contribute to the flame-retardant effect of

DP in the gas phase, because of the large amount of DOPO radicals (R and, mainly, S species of Fig. S5) produced during the pyrolysis process. The formation of a noticeable amount of flame inhibitors clearly indicates that a gas phase mechanism in combination with a strong condensed phase activity justify the very good performances in terms of fire behavior. In addition, the PEPA unit (T species of Table S3 and Fig. S5) of DP could also remain in the condensed phase to produce phosphoric acids, responsible for condensed phase activity, as already observed for different polymer matrices (i.e. polyesters) [17,48].

A simplified flame-retardant mechanism of DP is thus proposed in Scheme 1 and is based on the earlier discussed gas phase (Scheme S1) and condensed phase reactions. It is likely that most of the P-content of the residues might be arise from the retention of P from PEPA part of DP (which contributes ∼55% of the total P-content of DP) and that some retained phosphorus can be also contributed by the decomposition pathway of DOPO part. As shown in Scheme 1, DP decomposition generates PEPA units responsible for a further decomposition to polyphosphoric acid compounds during the combustion process [17]. It is reported in the literature that melamine undergoes endothermic decomposition (∼347 °C) producing N_2 and NH_3 [42,43]. NH_3 may react with some polyphosphoric acid produced in the course of DP degradation, leading to the formation of P-N-O polymeric substructures (i.e. phosphorus oxynitride) in the char. The formation of P-N-O species together with polyphosphoric acid in the condensed phase agrees with a higher P-content in the residue of **EPO_DP2P_Mel** and **EPO2Si_DP2P_Mel**, resulting in the synergistic interaction of melamine with DP.

On the basis of pictures shown in Fig. S3, S4, elemental analysis presented in Table S5 and the proposed mode of action of DP (Scheme 1), a combined effect of DP, melamine and silica nanoparticles (silicaNp) acting in the condensed and the gas phase of combustion process is proposed in Fig. 10. It is known that, epoxy resins are well-established charring-polymers, undergoing carbonization process during the combustion resulting a char dominated with C, H and N elements (Fig. 10a) [65]. Silica-epoxy nanocomposites begin to burn when the polymer matrix is heated to temperatures, at which thermal degradation begins. The degradation products are superheated and nucleated to form bubbles [53]. Fig. 10b shows that at these temperatures the bubbles burst at heated surfaces, evolving their contents as fuel vapor into the gas phase. Silica nanoparticles (silicaNp) in form of crosslinked network accumulate at material surfaces through a couple of possible mechanisms: the rising of bubbles during the combustion pushes the silicaNp to the material surface, while the polymer recesses from the material surface during pyrolysis, leaving behind the silicaNp [53]. The ceramic silica layer (Fig. 10b, Table S5) emits radiation from the material surface, impeding the transport of bubbles and heat, and acts as a thermal protective barrier against the decomposed gas supplied from the bulk polymer and against oxygen diffusing from the air into the material [54,66]. This mechanism describes the improved fire behavior for **EPO2Si** with respect to **EPO** observed in cone calorimetry (Table 3) [9]. The incorporation of DP in the epoxy (**EPO_DP2P**) results in the formation of a significantly higher amount of stable and coherent char due to the PEPA unit that produces polyphosphoric acid responsible for condensed phase activity (dehydration reactions) and earlier ignition (Fig. 10c and Table 3) [17–21, 48]. Additionally, as reported above, gas phase flame inhibition of DP contributes to the strong reduction of HRR (∼75%) compared to the pristine epoxy (Table 3, Scheme 1 and Scheme S1).

The presence of melamine together with DP in the epoxy (**EPO_DP2P_Mel**) may result in two phenomena (i.e. physical and chemical) in the condensed phase. During the endothermic degradation of melamine, some nitrogen-based volatiles are produced, which are mainly composed of NH_3 and nitrogen [43]. Nitrogen leads to a dilution in the gas phase (blue arrows, Fig. 10d), where the highest amount of flammable species is located, and causes intumescence (Fig. S4d) [42,49]. As reported in the literature [67], NH_3 may react with decomposition products of DP to produce P-N-O polymeric substructures (i.e.
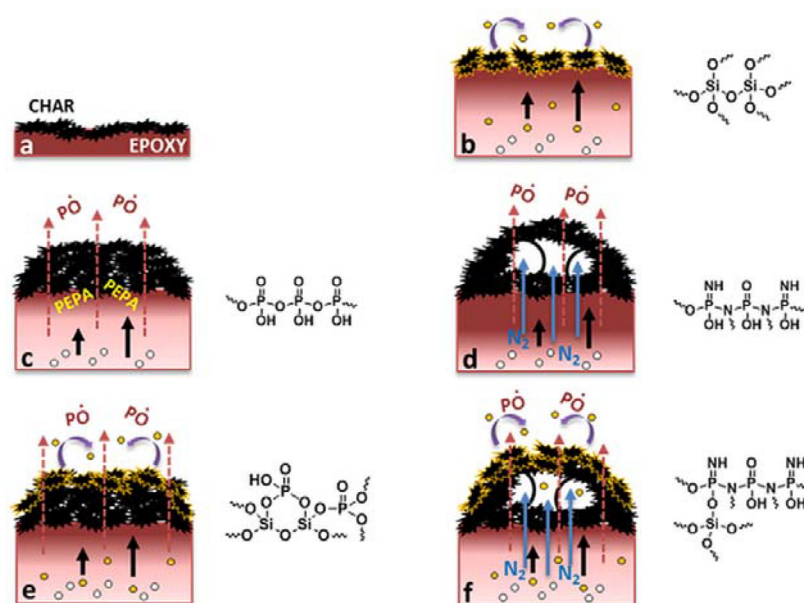
Fig. 10. Proposed mechanism of EPO/DP-Mel-silicaNp in oxygen (O_2) atmosphere. (a) **EPO**, (b) **EPO2Si**, (c) **EPO_DP2P**, (d) **EPO_DP2P_Mel**, (e) **EPO2Si_DP2P** and (f) **EPO2Si_DP2P_Mel**. The black arrows indicate the direction of the rising bubbles (white balls) from the hot bulk polymer matrix (pink region). The yellow circles represent the in-situ generated silica nanoparticles (silicaNp) in the epoxy resin. The yellow border line around the black char designates a ceramic silica layer (thermal shield and oxygen barrier) lying on the carbonaceous residue. The dark pink region depicts a zone where an advanced stage of decomposition for the polymer matrix occurs, because it is closer to the high decomposition surface char. The chemical formulas represent the polymeric substructures formed in the respective residue surface.
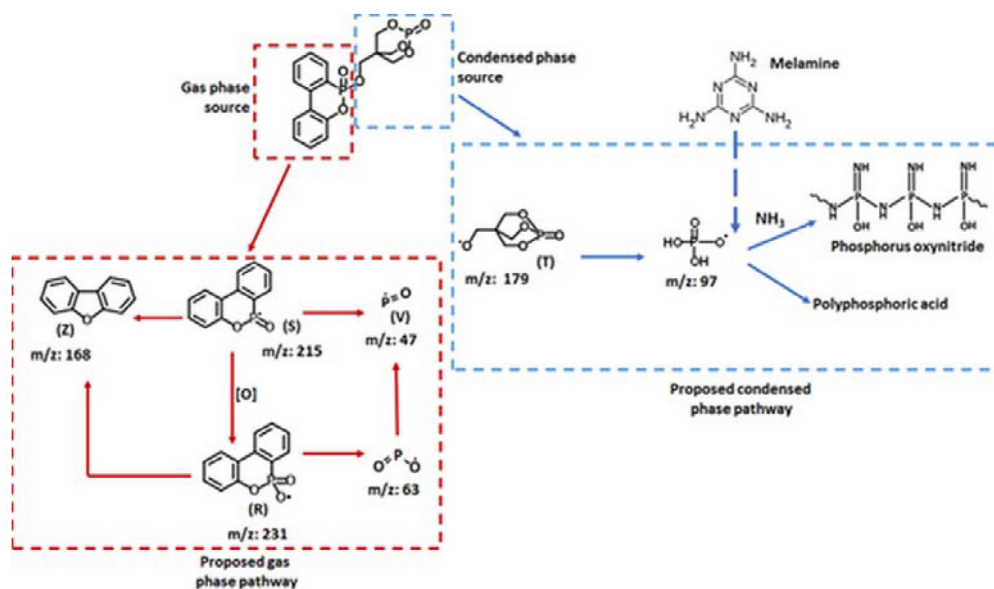
Scheme 1. Proposed pathways for gas phase and condensed phase mode of action of DP flame-retardant additive.

phosphorus oxynitride) as an insulating coating on the surface of the residue (Fig. 10d, Scheme 1). The clue to formation of this protective barrier is indicated by the presence of P, N and O, detection of P-N species in ATR-FTIR analysis and a higher retention of P in the residue of **EPO_DP2P_Mel** compared to **EPO_DP2P** (Table S5). This synergistic action of melamine results in a strong delay (~31%) of the ignition time (Table 3) possibly due to P–N–O char.

In the case of **EPO2Si_DP2P**, the silica-epoxy network degrades forming silica substructures [66,68]. During the combustion process the silanol groups of Si-O-Si polymeric species may condense with the decomposition products of DP (polyphosphoric acid), leading to the formation of ceramic thermal shield on a very abundant char (Fig. 10e and S4e) [69] and reducing the HRR and pHRR further (Table 3). Besides, **EPO2Si** and **EPO2Si_DP2P** show lower THR values than **EPO** in agreement with the thermal shielding exerted by the Si-O-Si and P-O-Si polymeric substructures respectively on the char.

The combined use of DP, silicaNp and melamine (**EPO2Si_DP2P_Mel**) allows the formation of an intumescent char

characterized by the presence of P-N-O-Si-O-P polymeric substructures on the surface [67,69]. The reaction between NH_3 and polyphosphoric acid produces P-N-O substructures which is able to condense with the silanol groups of Si–O–Si and P–O–Si polymeric species (Fig. 10f) to form a thermally stable char. Such char works as a thermal shield and oxygen barrier at the boundary layer [19–21, 54,55], leading to a higher retention of P for **EPO2Si_DP2P_Mel** compared to **EPO2Si_DP2P** (Table S5) and a strong delay in the ignition time (Table 3). Fig. S7 shows a noticeable amount of intumescent char produced after cone calorimeter test for **EPO2Si_DP2P_Mel** [68], which clearly indicates that a strong condensed phase mechanism exists which help achieve excellent performances in the UL 94 (V0 class flammability) and cone calorimetry tests, despite the use of an aliphatic amine as hardener (i.e. IPDA). The interaction of silica, phosphorus flame retardants and nitrogen additives to form a stable char and resulting in an improved fire performance is well known for other polymeric systems [67,68,70].
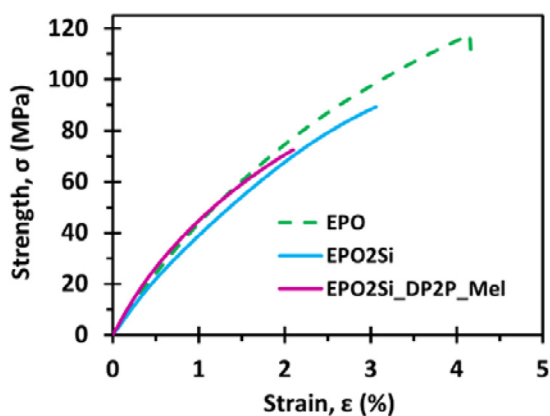
Fig. 11. Stress-strain curves obtained through tensile tests on **EPO**, **EPO2Si** and **EPO2Si_DP2P_Mel**.

3.7. Mechanical behavior

Tensile behavior of the pristine epoxy resin and in-situ silica-epoxy composites were investigated by following ASTM D638 standard (Table S6). In particular, the tensile modulus of **EPO, EPO2Si,** and **EPO2Si_DP2P_Mel** samples was estimated from the slope of stress-strain curve below 0.2% (Fig. 11). The presence of in-situ silica (**EPO2Si**) slightly lowered the Young's modulus and fracture strength compared to pristine epoxy (Table S6), as already noted in the literature [71]. The incorporation of silica also negatively affects the fracture toughness (U_T, Fig. 11). The inclusion of melamine and DP has a detrimental effect on the fracture energy of the composites, leading to a reduction of fracture strength and toughness (Table S6). Conversely, the addition of DP causes an increase of the Young modulus by more than 32%, probably due to a stiffness effect of DP, by decreasing the random motion of the epoxy chains through the formation of hydrogen bonds and polar interactions (see Section 3.2) [37,72,73].

4. Conclusions

Herein, an "in-situ" sol–gel synthesis of silica nano particles was performed in a commercial epoxy resin (DGEBA) and cured with a cycloaliphatic amine (isophorone diamine, IPDA). 6H-dibenz[c,e][1,2]oxaphosphorin,6-[(1-oxido-2,6,7-trioxa-1-phosphabicyclo[2.2.2]oct-4-yl)methoxy]-, 6-oxide (DP) as a hybrid flame-retardant (i.e. active in condensed and gas phase) and melamine as nitrogen source was added to the modified epoxy resin to improve the fire performance of the silica-epoxy nanocomposite. TGA analysis of the modified epoxy resin revealed that, the incorporation of DP strongly promotes the thermal oxidative stability of the epoxy system by boosting the char-forming process, thus leading to an increase in the residues at higher temperature. DP degradation releases PEPA units in the condensed phase to produce phosphoric acids which are responsible for a strong condensed phase activity. Furthermore, the presence of DP in the epoxy system prevents melt dripping during the vertical burning tests. UL 94 vertical flame spread tests supported by an IR camera revealed that the addition of DP in combination with melamine strongly improves the flame-retardant behavior of the silica-epoxy nanocomposites, where the flame propagation immediately stops during the first stages of the burning process. In particular, only for the formulation containing DP, melamine and silica nanoparticles a UL 94-V0 classification was at a low concentration of P (~2 wt %). PCFC and Cone Calorimetry results showed that the addition of DP and melamine to the in-situ silica-epoxy system has a significant positive effect on the HRC and promote a strong reduction in the HRR (up to 80%) values, together with an increase in the residue. Besides, the combined interaction of silica, DP and melamine catalyzes the forma-

tion of N–P–O–Si containing intumescent char, which acts as a thermal shield and oxygen barrier, which enables the epoxy system to achieve excellent fire performance. DIP-MS, cone calorimeter (CO/CO_2 ratio) and PY-GC-MS data supported a minor gas phase activity of DP linked to a flame inhibition mechanism. Increased char formation in TGA, PCFC and Cone calorimeter experiments and EDX analysis supported a dominant condensed phase activity of the additives. Finally, tensile results of the epoxy systems show that the presence of DP, silica nanoparticles and melamine resulted in a slight reduction in the fracture strength and toughness and a strong increase in the Young's modulus (~20%).

Thus, in this work we have demonstrated that by a simple combination of additives (hybrid flame-retardant, melamine and silica) it is possible to achieve excellent fire protection for epoxy resins cured with aliphatic hardener. In future, the combination of such flame-retardant additives in fire protection of DGEBA cured with other aliphatic hardeners and fully aliphatic epoxy systems will be explored.

Declaration of Competing Interest

The authors declare no conflict of interest.

Supplementary materials

Supplementary material associated with this article can be found, in the online version, at doi:10.1016/j.jcomc.2020.100022.

References

[1] F.L. Jin, X. Li, S.J. Park, Synthesis and application of epoxy resins: a review, J. Ind. Eng. Chem. 29 (2015) 1–11.
[2] S. Ambs, H.G. Neumann, Acute and chronic toxicity of aromatic amines studied in the isolated perfused rat liver, Toxicol. Appl. Pharm. 139 (1996) 186–194.
[3] W. Brostow, S.H. Goodman, J. Wahrmund, William Andrew Publishing, Boston, 2014, pp. 191–252.
[4] E. Weil, S. Levchik, A review of current flame retardant systems for epoxy resins, J. Fire Sci. 22 (2004) 25–40.
[5] P. Darnerud, Toxic effects of brominated flame retardants in man in wildlife, Environ. Int. 29 (2003) 841–853.
[6] Y. Saegusa, H. Fujimoto, G.H. Woo, K. Inoue, M. Takahashi, K. Mitsumori, M. Hirose, A. Nishikawa, M. Shibutani, Developmental toxicity of brominated flame retardants, tetrabromobisphenol A and 1,2,5,6,9,10-hexabromocyclododecane, in rat offspring after maternal exposure from mid-gestation through lactation, Reprod. Toxicol. 28 (2009) 456–467.
[7] K.K. Kefeni, J.O. Okonkwo, O.I. Olukunle, B.M. Botha, Brominated flame retardants: Sources, distribution, exposure pathways, and toxicity, Environ. Rev. 19 (2011) 238–253.
[8] J.J. Chruściel, E. Leśniak, Modification of epoxy resins with functional silanes, polysiloxanes, silsesquioxanes, silica and silicates, Prog. Polym. Sci. 41 (2015) 67–121.
[9] A. Bifulco, F. Tescione, A. Capasso, P. Mazzei, A. Piccolo, M. Durante, M. Lavorgna, G. Malucelli, F. Branda, Effects of post cure treatment in the glass transformation range on the structure and fire behavior of in situ generated silica/epoxy hybrids, J. Sol-Gel Sci. Technol. 87 (2018) 156–169.
[10] S.Y. Lu, I. Hamerton, Recent developments in the chemistry of halogen-free flame retardant polymers, Prog. Polym. Sci. 27 (2002) 1661–1712.
[11] K.A. Salmeia, S. Gaan, An overview of some recent advances in DOPO-derivatives: chemistry and flame retardant applications, Polym. Degrad. Stab. 113 (2015) 119–134.
[12] J. Passaro, P. Russo, A. Bifulco, M.T. De Martino, V. Granata, B. Vitolo, G. Iannace, A. Vecchione, F. Marulo, F. Branda, Water resistant self-extinguishing low frequency soundproofing polyvinylpyrrolidone based electrospun blankets, Polymers 11 (2019) 1205.
[13] B. Szolnoki, A. Toldy, P. Konrád, G. Szebényi, G. Marosi, Comparison of additive and reactive phosphorus-based flame retardants in epoxy resins, Period. Polytech. Chem. Eng. 57 (2013) 85–91.
[14] T.P. Ye, S.F. Liao, Y. Zhang, M.J. Chen, Y. Xiao, X.Y. Liu, Z.G. Liu, D.Y. Wang, Cu(0) and Cu(II) decorated graphene hybrid on improving fireproof efficiency of intumescent flame-retardant epoxy resins, Compos. Part B Eng. 175 (2019) 107189.

[15] W. Zhang, X. Li, R. Yang, Novel flame retardancy effects of DOPO-POSS on epoxy resins, Polym. Degrad. Stab. 96 (2011) 2167–2173.

[16] C. Hirsch, B. Striegl, C. Adlhart, M. Edelmann, E. Bono, S. Gaan, K. Salmeia, L. Hoelting, A. Krebs, J. Nyffeler, R. Pape, A. Bürkle, M. Leist, P. Wick, S. Schildknecht, Multiparameter toxicity assessment of novel DOPO-derived organophosphorus flame retardants, Arch. Toxicol. 91 (2016) 407–425.

[17] K.A. Salmeia, A. Gooneie, P. Simonetti, R. Nazir, J.-P. Kaiser, A. Rippl, C. Hirsch, S. Lehner, P. Rupper, R. Hufenus, Comprehensive study on flame retardant polyesters from phosphorus additives, Polym. Degrad. Stab. 155 (2018) 22–34.

[18] S.L. Waaijers, J. Hartmann, A.M. Soeter, R. Helmus, S.A.E. Kools, P. de Voogt, W. Admiraal, J.R. Parsons, M.H.S. Kraak, Toxicity of new generation flame retardants to Daphnia magna, Sci. Total Environ. 463 (2013) 1042–1048.

[19] M. Liu, H. Yin, X. Chen, J. Yang, Y. Liang, J. Zhang, F. Yang, Y. Deng, S. Lu, Preliminary ecotoxicity hazard evaluation of DOPO-HQ as a potential alternative to halogenated flame retardants, Chemosphere 193 (2018) 126–133.

[20] A. Gooneie, P. Simonetti, K.A. Salmeia, S. Gaan, R. Hufenus, M.P. Heuberger, Enhanced PET processing with organophosphorus additive: Flame retardant products with added-value for recycling, Polym. Degrad. Stab. 160 (2019) 218–228.

[21] Y. Zhang, B. Yu, B. Wang, K.M. Liew, L. Song, C. Wang, Y. Hu, Highly effective P–P synergy of a novel DOPO-based flame retardant for epoxy resin, Ind. Eng. Chem. Res. 56 (2017) 1245–1255.

[22] L. Matějka, K. Dušek, J. Pleštil, J. Kříž, F. Lednický, Formation and structure of the epoxy-silica hybrids, Polymer 40 (1999) 171–181.

[23] L. Matějka, O. Dukh, J. Kolařík, Reinforcement of crosslinked rubbery epoxies by in-situ formed silica, Polymer 41 (2000) 1449–1459.

[24] J. Marti, S.R. Idelsohn, E. Oñate, A Finite Element Model for the Simulation of the UL-94 Burning Test, Fire Technol. 54 (2018) 1783–1805.

[25] R. Stämpfli, P. Brühwiler, I. Rechsteiner, V. Meyer, R. Rossi, X-ray tomographic investigation of water distribution in textiles under compression – Possibilities for data presentation, Measurement 46 (2013) 1212–1219.

[26] H. Chen, J. Wang, A. Ni, A. Ding, X. Han, Z. Sun, The effects of a macromolecular charring agent with gas phase and condense phase synergistic flame retardant capability on the properties of PP/IFR composites, Materials 11 (2018) 111.

[27] R.R. Randle, D.H. Whiffen, The infra-red intensities of a band near 1020 cm–1 in mono-and para-substituted benzene derivatives, Trans. Faraday Soc. 52 (1956) 9–13.

[28] K.S. Tewari, N.K. Vishnoi, A Textbook of Organic Chemistry, Publishing House Pvt. Ltd., New Delhi, 1976 Vikas.

[29] L. Daasch, D. Smith, Infrared spectra of phosphorus compounds, Anal. Chem. 23 (1951) 853–868.

[30] M.A.A. Beg, H.C. Clark, Chemistry of the trifluoromethyl group: part v. Infrared spectra of some phosphorus compounds containing CF3, Can. J. Chem. 40 (1962) 393–398.

[31] S. Zhou, L. Song, Z. Wang, Y. Hu, W. Xing, Flame retardation and char formation mechanism of intumescent flame retarded polypropylene composites containing melamine phosphate and pentaerythritol phosphate, Polym. Degrad. Stab. 93 (2008) 1799–1806.

[32] S. Belov, G.T. Fraser, J. Ortigoso, B.H. Pate, M.Y. Tretyakov, Electric resonance optothermal spectrum of the 920 cm-1 v 14+ v 15 torsional combination band of acetaldehyde, Mol. Phys. 81 (1994) 359–368.

[33] V.B. Singh, Spectroscopic signatures and structural motifs in isolated and hydrated theophylline: a computational study, RSC Adv. 5 (2015) 11433–11444.

[34] S.S. Mahapatra, N. Karak, s-Triazine containing flame retardant hyperbranched polyamines: synthesis, characterization and properties evaluation, Polym. Degrad. Stab. 92 (2007) 947–955.

[35] K.A. Salmeia, A. Neels, D. Parida, S. Lehner, D. Rentsch, S. Gaan, Insight into the synthesis and characterization of organophosphorus-based bridged triazine compounds, Molecules 24 (2019) 2672.

[36] A. Bifulco, D. Parida, K.A. Salmeia, R. Nazir, S. Lehner, R. Stämpfli, H. Markus, G. Malucelli, F. Branda, S. Gaan, Fire and mechanical properties of DGEBA-based epoxy resin cured with a cycloaliphatic hardener: combined action of silica, melamine and DOPO-derivative, Mater. Des. 193 (2020) 108862.

[37] F. Wang, S. Pan, P. Zhang, H. Fan, Y. Chen, J. Yan, Synthesis and application of phosphorus-containing flame retardant plasticizer for polyvinyl chloride, Fibers Polym. 19 (2018) 1057–1063.

[38] R.F. Lange, E.W. Meijer, Supramolecular polymer interactions based on the alternating copolymer of styrene and maleimide, Macromolecules 28 (1995) 782–783.

[39] H. Yan, C. Lu, D. Jing, X. Hou, Chemical degradation of amine-cured DGEBA epoxy resin in supercritical 1-propanol for recycling carbon fiber from composites, Chin. J. Polym. Sci. 32 (2014) 1550–1563.

[40] N. Grassie, M.I. Guy, N.H. Tennent, Degradation of epoxy polymers. Part 1—products of thermal degradation of bisphenol-A diglycidyl ether, Polym. Degrad. Stab. 12 (1985) 65–91.

[41] P. Musto, G. Ragosta, P. Russo, L. Mascia, Thermal-oxidative degradation of epoxy and epoxy-bismaleimide networks: kinetics and mechanism, Macromol. Chem. Phys. 202 (2001) 3445–3458.

[42] K. Bretterbauer, C. Schwarzinger, Melamine derivatives-a review on synthesis and application, Curr. Org. Synth. 9 (2012) 342–356.

[43] G. Zhan, L. Zhang, Y. Tao, Y. Wang, X. Zhu, D. Li, Anodic ammonia oxidation to nitrogen gas catalyzed by mixed biofilms in bioelectrochemical systems, Electrochim. Acta 135 (2014) 345–350.

[44] L. Costa, G. Camino, Thermal behaviour of melamine, J. Therm. Anal. 34 (1988) 423–429.

[45] G. Malucelli, Surface-engineered fire protective coatings for fabrics through sol-gel and layer-by-layer methods: an overview, Coatings 6 (2016) 33.

[46] H. Singh, A.K. Jain, Ignition, combustion, toxicity, and fire retardancy of polyurethane foams: a comprehensive review, J. Appl. Polym. Sci. 111 (2009) 1115–1143.

[47] X. Liu, K.A. Salmeia, D. Rentsch, J. Hao, S. Gaan, Thermal decomposition and flammability of rigid PU foams containing some DOPO derivatives and other phosphorus compounds, J. Anal. Appl. Pyrolysis 124 (2017) 219–229.

[48] W. Zhang, X. He, T. Song, Q. Jiao, R. Yang, The influence of the phosphorus-based flame retardant on the flame retardancy of the epoxy resins, Polym. Degrad. Stab. 109 (2014) 209–217.

[49] S. Bourbigot, S. Duquesne, Fire retardant polymers: recent developments and opportunities, J. Mater. Chem. 17 (2007) 2283–2300.

[50] T.R. Crompton, Characteristics and Analysis of Non-flammable Polymers, Smithers Rapra Technology, Ltd., Shropshire, 2013.

[51] K. Salmeia, J. Fage, S. Liang, S. Gaan, An overview of mode of action and analytical methods for evaluation of gas phase activities of flame retardants, Polymers 7 (2015) 504–526.

[52] B. Schartel, Phosphorus-based flame retardancy mechanisms—old hat or a starting point for future development? Materials 3 (2010) 4710–4745.

[53] P.M. Visakh, Y. Arao, Flame Retardants: Polymer Blends, Composites and Nanocomposites, Springer, Berlin, 2015.

[54] T. Kashiwagi, F. Du, J. Douglas, K. Winey, H. Jr, J. Shields, Nanoparticle networks reduce the flammability of polymer nanocomposites, Nat. Mater. 4 (2006) 928–933.

[55] L. Jianjun, O. Yuxiang, Theory of Flame Retardation of Polymeric Materials, Walter de Gruyter GmbH & Co KG, Berlin, 2019.

[56] A.B. Morgan, J.W. Gilman, An overview of flame retardancy of polymeric materials: application, technology, and future directions, Fire Mater. 37 (2013) 259–279.

[57] S. Molyneux, A.A. Stec, T.R. Hull, The effect of gas phase flame retardants on fire effluent toxicity, Polym. Degrad. Stab. 106 (2014) 36–46.

[58] H. Yan, C. Lu, D. Jing, X. Hou, Chemical degradation of TGDDM/DDS epoxy resin in supercritical 1-propanol: promotion effect of hydrogenation on thermolysis, Polym. Degrad. Stab. 98 (2013) 2571–2582.

[59] A. Gooneie, P. Simonetti, K.A. Salmeia, S. Gaan, R. Hufenus, M.P. Heuberger, Enhanced PET processing with organophosphorus additive: Flame retardant products with added-value for recycling, Polym. Degrad. Stab. 160 (2019) 218–228.

[60] P. Wang, F. Yang, L. Li, Z. Cai, Flame-retardant properties and mechanisms of epoxy thermosets modified with two phosphorus-containing phenolic amines, J. Appl. Polym. Sci. 133 (2016) 43953.

[61] S.T. Cholake, M.R. Mada, R.K.S. Raman, Y. Bai, X.L. Zhao, S. Rizkalla, S. Bandyopadhyay, Quantitative analysis of curing mechanisms of epoxy resin by mid and near-fourier transform infra red spectroscopy, Def. Sci. J. 64 (2014) 314–321.

[62] A. Bifulco, A. Marotta, J. Passaro, A. Costantini, P. Cerruti, G. Gentile, V. Ambrogi, G. Malucelli, F. Branda, Thermal and fire behavior of a bio-based epoxy/silica hybrid cured with methyl nadic anhydride, Polymers 12 (2020) 1661.

[63] R. Jian, P. Wang, W. Duan, J. Wang, X. Zheng, J. Weng, Synthesis of a novel P/N/S-containing flame retardant and its application in epoxy resin: thermal property, flame retardance, and pyrolysis behavior, Ind. Eng. Chem. Res. 55 (2016) 11520–11527.

[64] L.K. Nait-Ali, X. Colin, A. Bergeret, Kinetic analysis and modelling of PET macromolecular changes during its mechanical recycling by extrusion, Polym. Degrad. Stab. 96 (2011) 236–246.

[65] H. Marsh, F.R. Reinoso, Activated Carbon, Elsevier Science, London, 2006.

[66] T. Kashiwagi, F. Du, K.I. Winey, K.M. Groth, J.R. Shields, S.P. Bellayer, H. Kim, J.F. Douglas, Flammability properties of polymer nanocomposites with single-walled carbon nanotubes: effects of nanotube dispersion and concentration, Polymer 46 (2005) 471–481.

[67] S. Gaan, G. Sun, K. Hutches, M.H. Engelhard, Effect of nitrogen additives on flame retardant action of tributyl phosphate: phosphorus–nitrogen synergism, Polym. Degrad. Stab. 93 (2008) 99–108.

[68] J.W. Gilman, R.H. Harris, J.R. Sheilds, T. Kashiwagi, A.B. Morgan, A study of the flammability reduction mechanism of polystyrene-layered silicate nanocomposite: Layered silicate reinforced carbonaceous char, Polym. Adv. Technol. 17 (2006) 263–271.

[69] Q. Li, P. Jiang, Z. Su, P. Wei, G. Wang, X. Tang, Synergistic effect of phosphorus, nitrogen, and silicon on flame-retardant properties and char yield in polypropylene, J. Appl. Polym. Sci. 96 (2005) 854–860.

[70] Q. Dong, M. Liu, Y. Ding, F. Wang, C. Gao, P. Liu, B. Wena, S. Zhanga, M. Yanga, Synergistic effect of DOPO immobilized silica nanoparticles in the intumescent flame retarded polypropylene composites, Polym. Advan. Technol. 24 (8) (2013) 732–739.

[71] B.B. Johnsen, A.J. Kinloch, R.D. Mohammed, A.C. Taylor, S. Sprenger, Toughening mechanisms of nanoparticle-modified epoxy polymers, Polymer 48 (2007) 530–541.

[72] G. Luciani, A. Costantini, B. Silvestri, F. Tescione, F. Branda, A. Pezzella, Synthesis, structure and bioactivity of pHEMA/SiO2 hybrids derived through in situ sol–gel process, J. Sol-Gel Sci. Technol. 46 (2008) 166–175.

[73] H.C. Erythropel, S. Shipley, A. Börmann, J.A. Nicell, M. Maric, R.L. Leask, Designing green plasticizers: influence of molecule geometry and alkyl chain length on the plasticizing effectiveness of diester plasticizers in PVC blends, Polymer 89 (2016) 18–27.